ORIGINAL PAPER

JMS Journal of Medical Science

Gold nanoparticles capped with sulfamethoxazole-ovotransferrin conjugate as a potential nanomedicine for the treatment of microbial infections

Hisham R. Ibrahim
Department of Biochemistry and Biotechnology, Faculty of Agriculture, Kagoshima University, Kagoshima, Japan
https://orcid.org/0000-0002-7809-900X
Corresponding author: k2504042@kadai.jp

Takemichi Kubo
Department of Biochemistry and Biotechnology, Faculty of Agriculture, Kagoshima University, Kagoshima, Japan
–

https://doi.org/10.20883/medical.e1369

Keywords: Ovotransferrin, gold nanoparticles, drug-delivery, sulfamethoxazole, antibiotic, antibacterial, intracellular infection

Received 2025-07-29
Accepted 2025-10-14
Published 2025-12-29

How to Cite: Ibrahim HR, Kubo T. Gold nanoparticles capped with sulfamethoxazole-ovotransferrin conjugate as a potential nanomedicine for the treatment of microbial infections. Journal of Medical Science. 2025 December;94(4);e1369. doi:10.20883/medical.e1369

ABSTRACT

Introduction. Although sulfonamide antibiotics are potent antimicrobial agents against bacterial infections, their water insolubility and toxicity at high doses limit their therapeutic efficacy. This study explores a potent anti-infection drug-delivery system using gold nanoparticles (gNPs) capped with ovotransferrin (OTf) as a targeting carrier and solubilising agent for sulfamethoxazole (SMZ) antibiotic.

Materials and methods. The OTf was conjugated with sulfamethoxazole OTf(SMZ) at pH 9.0 for 24 h at 29°C. The conjugate (OTf(SMZ)) or free OTf was added to the gold chloride solution containing sodium citrate as a reducing agent, and then stirred for 24 h at 37˚C. The gold nanoparticle (GNP) formulations were purified by gel filtration. The gNP formulations and their individual components (free OTf, SMZ, and gNP tested separately) were evaluated against several microbial strains, including drug-resistant Salmonella, and against bacteria that infect human cells intracellularly.

Results. The gold nanoparticle capped with OTf loaded with SMZ [OTf(SMZ)-gNP] showed superior microbicidal activity against several bacterial strains and the fungi *Candida albicans* compared to the activities of gNP capped with OTf alone [OTf-gNP] or the individual agents. The wild-type *Salmonella* enteritidis, which encodes the multidrug efflux channel TolC, becomes susceptible to both OTf(SMZ)-gNP and OTf-gNP nanoformulation but not to their separate components. However, the *tolC*-knockout *Salmonella* enteritidis mutant strain was susceptible only to the OTf(SMZ)-gNP, indicating the ability of this nanoformulation to deliver the antibiotic SMZ into bacterial cells through self-promoted uptake. The OTf(SMZ)-gNP efficiently killed pathogens intracellularly infecting human colon carcinoma cells.

Conclusions. The results demonstrate that OTf(SMZ)-gNP nanomaterials can mediate the endocytosis of SMZ, making them suitable for targeting bacterial infections, including those that have acquired antibiotic resistance. The study highlights the potential of OTf-capped nanomaterials that can be engineered to enhance the potency of hydrophobic antibiotics for treating infectious diseases.

Introduction

Although many antibiotics, such as sulfonamides, have been effective in treating bacterial infections, antibiotic resistance remains a public health concern. This concern thus urges the development of a new strategy to combat bacterial infections. Sulfamethoxazole (SMZ) is a sulfonamide antibiotic used to treat a variety of infections with a broad antimicrobial spectrum, where it is effective against both gram-negative and gram-positive bacteria [1]. The mechanism of SMZ action involves inhibiting the production of the dihydrofolate intermediate, which interferes with the normal bacterial synthesis of folic acid, an essential component for bacterial growth and replication. Sulfonamide drugs can potentially cause allergic and toxic effects, and the factors influencing the toxicity include the dosage of the drug and its low solubility in blood [4]. The relatively poor water solubility of SMZ may contribute to toxicity due to the high concentration of acetylated groups. Therefore, drug-targeting is a practical approach in reducing allergenicity and toxicity, as the dosage of the drug can be reduced, and its efficacy is locally enhanced around the site of infection.

In a previous study, SMZ was rendered completely water-soluble by loading it into the molecule of ovotransferrin (OTf), and the OTf(SMZ) conjugate proved to be more potent antimicrobial than the individual components (free OTf, SMZ, and gNP) when tested separately, even against the antibiotic-resistant *Salmonella enteritidis* strain [5]. Furthermore, OTf has been proven effective in targeting anticancer drugs to colon and breast cancer cells through the transferrin receptor (TfR) [6]. However, the amount of drug that could be internalised into bacterial or infected cells was limited by the number of OTf-TfR complexes. Consequently, it may become necessary to make adjustments in dosing regimens of the drug by using nanoparticles, which have been considered valid for high drug loading [7]. Metallic nanoparticles have been studied as antibiotic carriers, including gold, silver, copper, titanium and zinc metal nanoparticles, which can penetrate intracellularly and exert antimicrobial properties [8,9].

It has been reported that gold nanoparticles exhibit direct permeation across cell membranes compared to other materials [10. Nanoparticle translocation across the cell membrane has been reported to occur through two pathways: endocytosis and direct diffusion [8]. The nanoparticle binds receptors in the membrane via multivalent interactions and captures several tens of receptors at any point [11]. By doing so, the particle deforms the membrane underneath it, thereby improving the therapeutic index of the drug payload compared to free drugs. Direct administration of antibiotics faces various barriers which prevent effective localisation of the antibiotic and reduce its retention [5]. An approach to overcome poor antibiotic retention and promote its effective localisation to the pathogen is to integrate nanoparticles with cell-targeted drug delivery systems.

In this study, we investigate the development of an effective drug-targeting strategy to deliver the water-insoluble SMZ directly to pathogens or intracellularly infected mammalian cells. Specifically, this study aimed to develop and characterise gold nanoparticles coated with the OTf(SMZ) complex as a targeted antibiotic delivery system and to evaluate their efficacy against resistant bacterial strains and intracellular infections. The strategy involves loading SMZ into the OTf molecule and then tagging gold nanoparticles with the SMZ-OTf conjugate. Most pathogens, as well as human epithelial cells, are known to express the transferrin receptor (TfR) and selectively take up OTf [5]. Thus, the SMZ-OTf conjugate is directly localised to pathogens or to the cells in which they reside. Therefore, while nanoparticles promote direct diffusion, effective dosage, and retention of the drug, they may also help alleviate antibiotic resistance. Through this approach, the gold nanoparticle SMZ-OTf demonstrated the ability to specifically deliver a high dose of antibiotics to, thereby overwhelming the efflux pumps that expel antibiotics from drug-resistant wild-type *Salmonella enteritidis* cells.

Materials and methods

Materials

Ovotransferrin, purchased from Inovatech Bio-Products Inc. (Abbotsford, Canada), was recrystallised and purified chromatographically using a Sephadex G-50 column (G5080). Sulfame-

thoxazole, SMZ (31737), gold chloride trihydrate, $HAuCl_4 \cdot 3H_2O$ (520918), fetal bovine serum, FBS (TMS-013), and trypan blue, TB (T6146), were from Sigma (St. Louis, MO). McCoy 5a medium (16600082) was from Invitrogen, Japan. CellTiter-Blue cell viability assay (G8080) was from Promega, Japan. Brain Heart Infusion, BHI (05509), trypticase soy broth, TSB (05518), and nutrient agar (05514) were obtained from Nissui (Tokyo, Japan). Unless otherwise specified, all other reagents were of analytical grade.

Microorganisms and cell lines

Microorganisms used for antimicrobial assays, *Salmonella enteritidis* (IFO 3313) and *Escherichia coli* K-12 (IFO 3301), were obtained from the Institute of Fermentation, Osaka, Japan. *Staphylococcus aureus* (NBRC 14462) and *Corynebacterium minutissimum* (NBRC 15361) were from the Nite Biological Resource Centre (Tokyo, Japan). *Propionibacterium acnes* (ATCC 6919), *Candida albicans* (ATCC 2091), and *Staphylococcus epidermidis* (ATCC 12228) were from the American Type Culture Collection (Rockville, MD, USA). The wild strain of *Streptococcus zooepidemicus* was obtained from the Institute of Bacteriology of the Veterinary Hospital, Zürich (Switzerland). The virulent wild-type of *Salmonella enterica* serotype Enteritidis phage type 4 strain 147 (147^{str}), originally isolated from egg content [12]. The *tol*C-deficient mutant *Salmonella Enteritidis* 147^{str} strain (Δ*tol*C), prepared by a one-step inactivation method [13], was a gift from the Department of Pathology, Bacteriology, and Avian Diseases, Faculty of Veterinary Medicine, Ghent University, Belgium.

Cell lines

Human colon carcinoma cell line HCT-116 (ATCC# CCL-247) from American Type Culture Collection (Rockville, MD) were maintained in McCoy's 5a media with 10% fetal bovine serum (FBS) and antibiotics (penicillin and streptomycin) at 37˚C in a humidified incubator with 5% CO_2. The medium was changed every other day.

Methods

Preparation of SMZ-OTf gold nanoparticle conjugate

Conjugation of OTf with sulfamethoxazole OTf(SMZ) was prepared as previously described [5]. Briefly, a freshly prepared antibiotic stock solution in 50% ethanol was added to the OTf solution to achieve a 60-fold molar excess of antibiotic over OTf in distilled water at pH 9.0, with stirring for 24 h at 29°C. The concentration of OTf in the mixture was 0.864 mg/mL. The prepara-

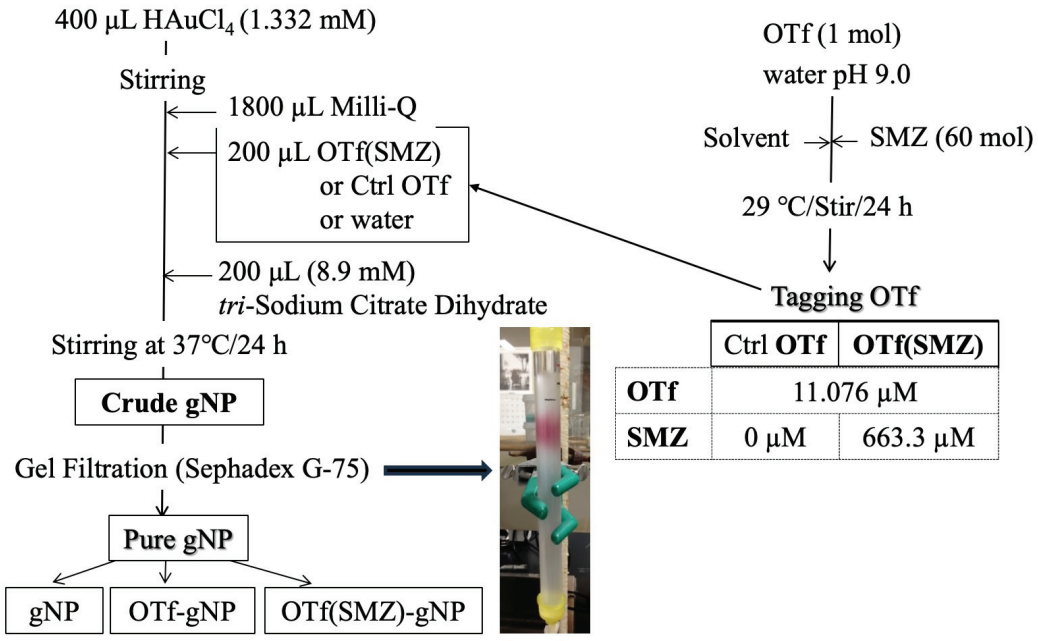

Scheme 1. Preparation of the OTf-SMZ tagged gNP. Concentration of OTf(SMZ) and control OTf are adjusted to 0.864 mg/mL (OTf- based).

tions were referred to as OTf(SMZ) complex and control (Ctrl OTf). Ctrl OTf was treated similarly except without an antibiotic.

To a 400 µL gold chloride solution (1.332 mM), 200 µL of 11.076 µM OTf(SMZ) or Ctrl OTf were added to 1800 µL Milli-Q water. For gold nanoparticles alone (gNP), water pH 9.0 was added. After adding 200 µL of sodium citrate dihydrate (8.9 mM) as a reducing agent, the mixture was stirred for 24 h at 37°C. This crude GDP formulation was purified by passing it through a gel-filtration column on Sephadex G-75. The molar ratio of gold chloride to OTf was 120:1 (mol/mol) in the respective OTf-tagged gold nanoparticle formulation. The gold nanoparticle formulations tagged with the OTf(SMZ) conjugate, OTf, or lacking the tag molecule were referred to as OTf(SMZ)-gNP, OTf-gNP, and gNP, respectively. The preparation procedure is detailed in **Scheme 1**.

Loading efficiency of SMZ into OTf(SMZ)-tagged gNPs

The crude gNP formulations were subjected to centrifugation at 15,000 × g for 30 min, and the supernatant was used to evaluate the SMZ loading efficiency onto OTf(SMZ)-gNPs. The total amount of free SMZ in the supernatant was determined spectrophotometrically at a maximum wavelength of 262 nm and quantified with an absorption molar coefficient of 11400 mol^{-1} L cm^{-1} [14]. The following equation was applied to calculate the loading efficiency:

$$\text{Loading efficiency (\%)} = [(\text{total SMZ} - \text{free SMZ}) / \text{total SMZ}] \times 100$$

Ultraviolet-visible light absorption spectrum analysis

To measure the adsorption of substances on the surface of the gNP preparations, the surface plasmon resonance peak unique to gNPs was measured using a SmartSpec-3000 spectrophotometer (Bio-Rad, USA). 150 150-µl of each sample was added to a quartz cell with an optical path length of 1.0 cm, and measurements were taken in the wavelength range of 300–800 nm.

Binding of OTf to gNPs

The confirmation of OTf incorporation into gNPs was verified by SDS-polyacrylamide gel electrophoresis (SDS-PAGE). Proteins that bind to the nanoparticle surface were isolated using the method of Saptarshi et al. [15]. Briefly, OTf-gNP preparation was denatured with 2-mercaptoethanol and centrifuged to recover the total OTf into the supernatant (Total OTf). Another portion of each preparation was centrifuged at 10,000 rpm for 10 minutes to remove the unbound OTf. The precipitate was denatured with 5% 2-mercaptoethanol (equal to the original volume) and centrifuged again to recover the bound OTf into the supernatant (Bound OTf), and the precipitate was the gNP. The precipitated gNP was washed with 5% 2-mercaptoethanol and centrifuged again to confirm recovery of all bound OTf into the supernatant (Wash). The collected supernatants were run on a 4% separation gel and a 15% concentration gel, at currents of 10 mA and 25 mA, respectively. After electrophoresis, the gel was stained with Coomassie Brilliant Blue (CBB) and destained with a 20:10:70 (v/v/v) methanol: acetic acid: water solution.

Transmission (TEM) and scanning (SEM) electron microscopy analysis

The size and shape of the formulated nanoparticles were analysed using a JEM-3010 transmission electron microscope (JEOL, Japan). A 2-µL sample was dropped onto a mesh and dried in a desiccator at room temperature for 24 hours. The acceleration voltage was 200 kV, and observations were made at magnifications of 20,000x and 100,000x. Particle diameter was determined from the images by comparing the measured data of 10 randomly selected particles with the scale bar length value. The average particle diameter of the nanoparticles was statistically calculated based on image data obtained at high magnification, and all values are presented as the mean value ± standard deviation (SD; n = 10). The morphology of nanoparticles was characterised using a SU-70 scanning electron microscope (SEM) operated at 15 kV (Hitachi High-Tech, Japan).

Antibacterial assay

The antibacterial activity of the nanoparticles against *Staphylococcus aureus, Staphylococcus epidermidis*, *Streptococcus zooepidermicus*, *Corynebacterium minutissimum*, *Propionibacterium acnes*, *Escherichia coli*, *Salmonella enteritidis* (wild-type), and *tol*C-deficient mutant

Salmonella enteritidis (Δ*tolC*) was tested using a liquid medium method. The mid-logarithmic phase cells, grown in brain heart infusion (BHI) broth, were washed and resuspended (to give 10^6 ~ 10^7 CFU/mL) in 1% trypticase soya broth (TSB), pH 7.3. Each inoculum was mixed with an equal volume of nanoparticle preparations, SMZ alone, or OTf equivalent to their contents in the respective nanoparticle. After incubation at 37°C for 24 h, a 30-µl portion or dilutions in physiological saline were spotted in triplicate onto a nutrient agar plate. The colony-forming units (CFU) were obtained after incubating agar plates at 37°C for 18 hours.

For *Candida albicans*, the blastoconidia grown at 28˚C for 36 h in 1% TSB, pH 7.3, were washed, resuspended (to a 10^6 ~ 10^7 CFU/mL) in Sabouraud dextrose broth (SAB) and mixed with an equal volume of nanoparticles or SMZ or OTf equivalent to their concentration in each derivative. After a 24-hour incubation at 28˚C, the mixture was plated on SAB agar. The plates were incubated for 24 h at 30°C, and the colonies were counted. All results are expressed as log CFU/mL as a function of OTf concentration in the assay medium of three independent experiments.

Intracellularly infected human cells

To elucidate the ability of OTf(SMZ)-gNP to deliver SMZ to intracellularly residing bacteria, human colon epithelial carcinoma cells, HCT-116, were infected with *Staphylococcus aureus* or *Escherichia coli,* and the intracellular bacteria were counted on agar plates. Briefly, Bacteria were grown in TSB broth at 37˚C for 20 h. The bacteria were washed twice and suspended in PBS buffer (pH 7.4). HCT-116 cells were seeded at 5 × 10^4 cells/well in 96-well plates in McCoy's 5A medium until they reached 80% confluence. Bacteria were adjusted to $10^{\wedge 4\text{-}10^{\wedge 5}}$ CFU/mL in PBS buffer and added to HCT-116 cells, which were then incubated at 37˚C under 5% CO_2. After 2 hours, the medium was replaced with McCoy's 5A containing 100 µg/mL gentamicin and incubated for 1 hour to kill extracellularly adherent bacteria. The cells were then washed three times with PBS and treated with medium containing nanoparticle derivatives (100 µg/mL final concentration, OTf-based) or their OTf and SMZ equivalents, and incubated for two h at 37˚C under 5% CO_2. Cells were lysed by adding 0.8 mL of 1% Triton X-100 in PBS for 15 minutes. A portion of suspension was serially diluted with sterilised physiological saline and spotted in triplicate on TSA agar. The plates were incubated for 24 hours at 37°C, and the colony-forming units (CFU) were calculated. The results are expressed as (log CFU/10^6 cells) of two independent experiments with three wells for each derivative.

In a clear-bottom, black 96-well plate, three wells were treated similarly for each sample used in the HCT-116 cell viability assay. Cell viability was determined using the fluorescent CellTiter-Blue Assay (Promega). The results are expressed as the percentage of cell viability relative to the control. The data are presented as the mean ± SD.

Statistical analysis

Experiments were carried out in duplicate or triplicate, and mean values were used for statistical analysis. Data obtained in the study were analysed statistically using one-way ANOVA by Excel's data analysis tools. Data shows mean values, and error bars show standard deviations.

Results

Synthesis of gold nanoparticles (gNP) capped with OTf and its SMZ complex

The OTf-capped [OTf-gNP] or OTf(SMZ)-capped [OTf(SMZ)-gNP] gold nanoparticles were synthesised by the redox method at ambient temperature using sodium citrate, as outlined in **Scheme 1**. Colourimetric shift in the UV-VIS region (300-800 nm) of the formed gNPs was employed to probe incorporation of OTf onto the gNP core shell (**Figure 1**). Due to the surface plasmon resonance of colloidal gold, the absorbance peak exhibits a variation in λmax depending on the size of the nanoparticles [16]. The absorbance peak of the pure gNP was observed at a maximum of 535 nm. The incorporation of OTf [OTf-gNP] resulted in a red shift in the spectra band from λmax of 535 to 538 nm. While OTf loaded with SMZ [OTf(SMZ)-gNP] resulted in a broader peak with red shift of λmax from 537 to 554 nm. The colour change (inset photos) and red shift of the surface plasmon resonance are characteristics of an increase in the gNP size, where the red shift correlates more strongly with the size [17]. These changes in

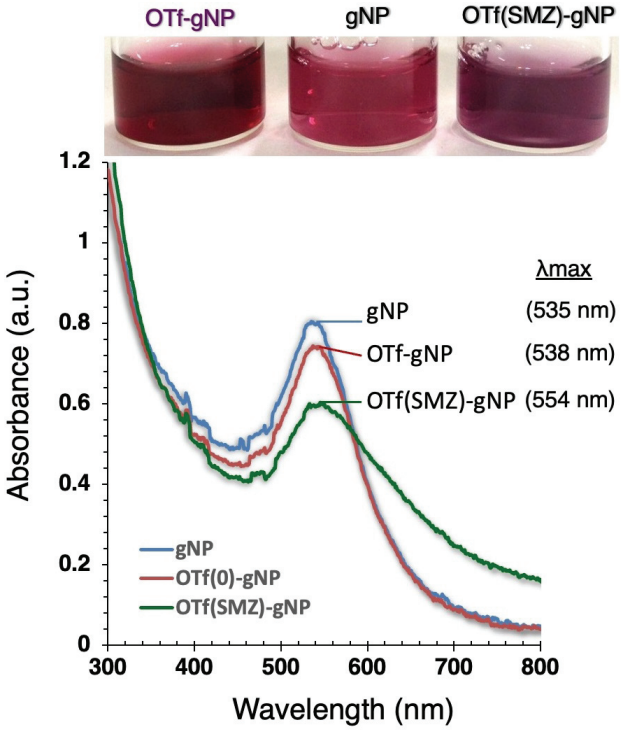

Figure 1. UV-VIS absorption spectra of gold nanoparticles synthesised in sodium citrate in the absence (gNP) and presence of OTf (OTf-gNP) or SMZ-loaded OTf (OTf(SMZ)-gNP). Each spectrum represents 24 24-hour reaction times. The inset photo shows the colour of nanoparticles formed in each preparation.

λmax suggested the formation of nanoparticles with a larger diameter. The λmax of OTf(SMZ)-gNP was shifted to a higher wavelength (red shift) and showed a broader peak, which could be attributed to the formation of larger particle sizes. The size and morphology of the nanoparticles were further characterised by transmission electron microscopy (TEM) and scanning electron microscopy (SEM) techniques (**Figure 2**). The addition of OTf or OTf(SMZ) increased the diameters of the nanoparticles. As shown in **Figure 2**, the particles were multi-dimensional, and the mean diameters of gNP (A), OTf-gNP (B), and OTf(SMZ)-gNP (C) nanoparticles were 15.72, 1.71, 19.32, 3.76, and 19.76, ±3.53 nm, respectively. The sizes of particles ranged between maximum diameters of 19.0 nm, 28.0 nm, and 24.0 nm to minimum diameters of 13.6 nm, 14.4 nm, and 13.0 nm for gNP, OTf-gNP, and OTf(SMZ)-gNP, respectively. The particles in all formulations were irregularly shaped, quasi-spherical, with most of the particles being spherical or ellipsoid in shape (**Figure 2**, inset images). Densitometric analysis of SDS-PAGE of the OTf-gNP nanoparticles (**Figure 3**) indicated that 36.29% of the total OTf is absorbed to the gNP, whereas 20.1% is monomer and 16.19% an aggregated form of bound OTf.

The determination of the loading efficiency of SMZ onto OTf(SMZ)-gNP confirmed a significant loading efficiency of ~68%. Initially, 168 µg/mL of SMZ was used in the formulation mixture, and 114 µg/mL of the SMZ remained attached to 0.84 mg/mL OTf.

Antibacterial activity of OTf(SMZ)-capped gold nanoparticles

We tested the bactericidal activities of the gold nanoparticle preparations against different bacterial strains (*Staphylococcus epidermidis*, *Staphylococcus aureus*, *Streptococcus zooepidemicus*, *Corynebacterium minutissimum*, *Propionibacterium acnes*, *Candida albicans*, *Escherichia coli* K-12, and *Salmonella enteritidis*). The activity was expressed as log CFU/mL as a function of OTf concentration in the nanoparticles. Free OTf and SMZ were tested at equivalent concentrations as in the nanoparticles. As shown in **Figure 4**, the OTf(SMZ)-gNP exhibited vigorous bacteri-

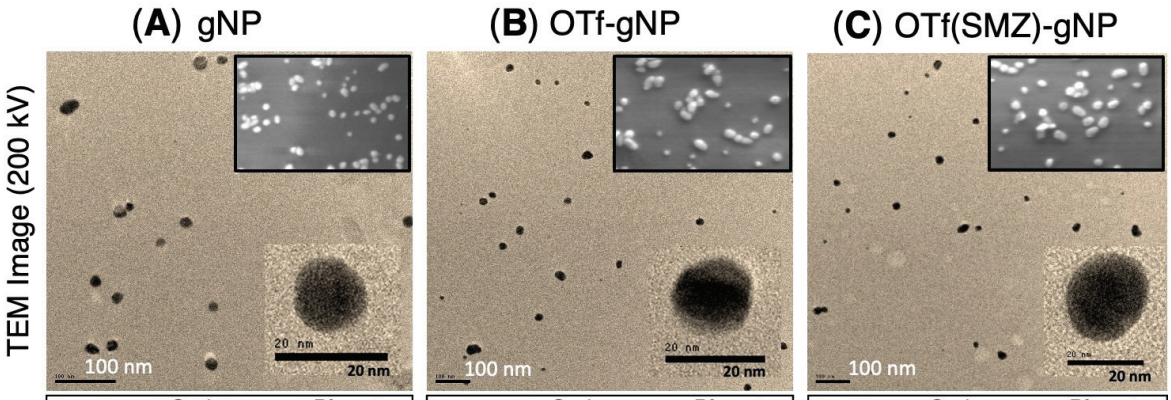

No.	Mag.	Scale bar	Scale	Diameter (nm)
1	100k	20	8.2	16.4
2	100k	20	7.5	15
3	100k	20	7.5	15
4	100k	20	7.3	14.6
5	100k	20	6.8	13.6
6	100k	20	7	14
7	100k	20	8	16
8	100k	20	9.5	19
9	100k	20	9	18
10	100k	20	7.8	15.6
Mean (nm)				**15.72**
SD				1.71
Max (nm)				19
Min (nm)				13.6

No.	Mag.	Scale bar	Scale	Diameter (nm)
1	100k	20	8.8	17.6
2	100k	20	9	18
3	100k	20	8.9	17.8
4	100k	20	7.2	14.4
5	100k	20	8.2	16.4
6	20k	100	1.8	18
7	20k	100	2	20
8	20k	100	2.2	22
9	20k	100	2.8	28
10	20k	100	2.1	21
Mean (nm)				**19.32**
SD				3.76
Max (nm)				28
Min (nm)				14.4

No.	Mag.	Scale bar	Scale	Diameter (nm)
1	100k	20	11	22
2	100k	20	10.8	21.6
3	25k	100	2	20
4	25k	100	2.2	22
5	25k	100	2.1	21
6	25k	100	2	20
7	25k	100	2.4	24
8	25k	100	1.4	14
9	25k	100	1.3	13
10	25k	100	2	20
Mean (nm)				**19.76**
SD				3.53
Max (nm)				24
Min (nm)				13

Figure 2. Nanoparticle morphology represented by TEM images of gNP (A), OTf-gNP (B) and OTf(SMZ)- gNP (C), as well as their SEM images (inset). Nanoparticle diameters of randomly selected ten particles, along with their mean diameters, are shown below the pictures. It can be seen that the gold nanoparticles are irregularly shaped, quasi-spherical, and within the nano-size range.

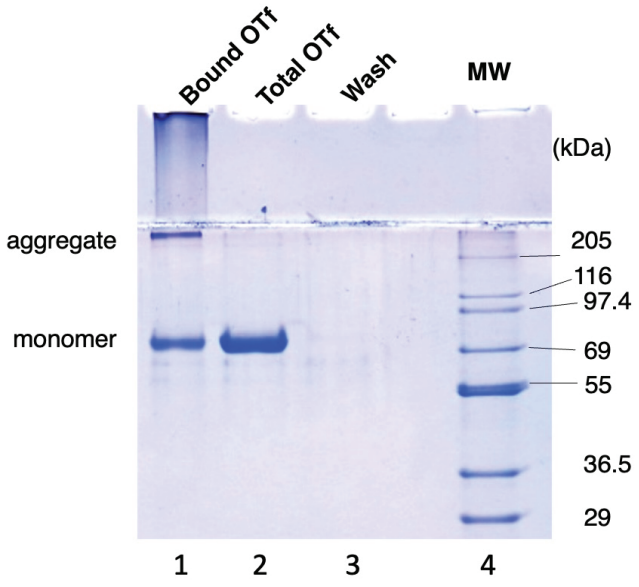

Figure 3. SDS-PAGE of OTf protein coronas formed in OTf-gNP formulation. Lane 1 is the tightly bound OTf to gNP. Lane 2 is the total OTf (free and bound OTf). Lane 3 confirms the total dissociation of OTf. Lane 4 is a protein marker.

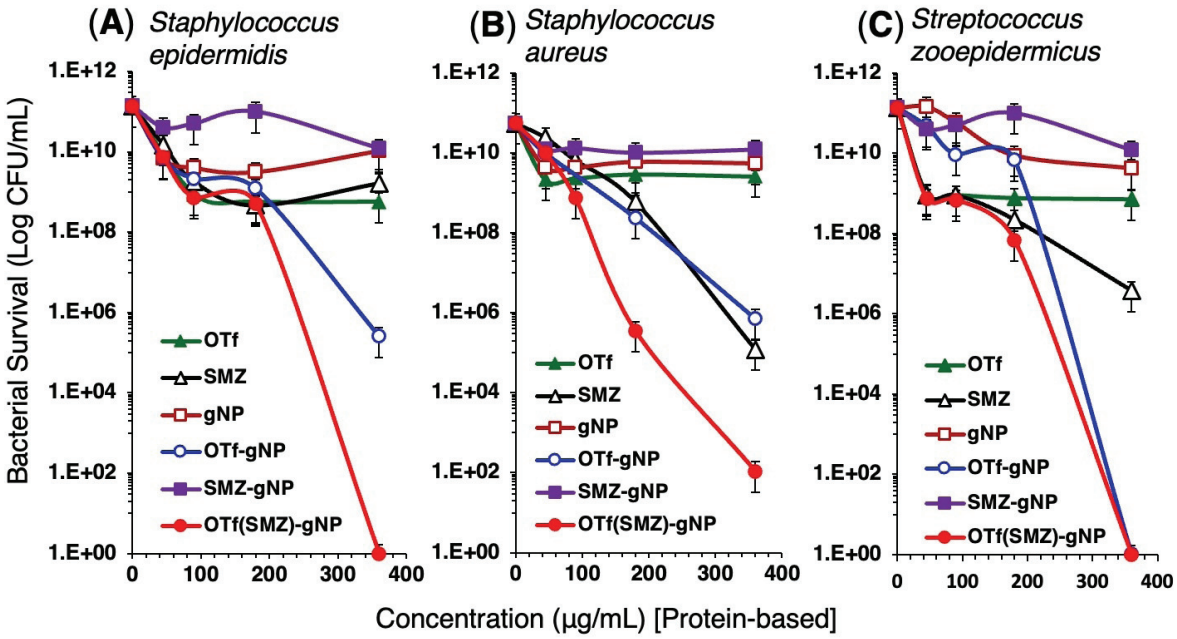

Figure 4. Bactericidal activity of various gNP formulations against three Gram-positive bacteria. The assay was performed against *Staphylococcus epidermidis* (A), *Staphylococcus aureus* (B), and *Streptococcus zooepidemicus* (C) at different doses of gNPs, as well as free SMZ and OTf at concentrations equivalent to their content in the respective formulations. The data is presented as log CFU/mL.

cidal activity, whereas severely reduced survival of the Gram-positive *Staphycoccus epidermidis* (A), *Staphycoccus aureus* (B), and *Streptococcus zooepidermicus* (C) in a dose-dependent manner. Interestingly, the OTf-gNP lacking the antibiotic exhibited remarkable dose-dependent bactericidal activity against the three strains, albeit weaker than that of OTf(SMZ)-gNP. Although free OTf and SMZ exhibited bactericidal activities, they were much weaker than OTf-gNP and OTf(SMZ)-gNP, and the effectiveness of the free OTf and SMZ varied depending on the strain.

We next tested the bactericidal activity against three strains of skin pathogens: *Corynebacterium minutissimum* (A), *Propionibacterium acnes* (B) and the fungus *Candida albicans* (C), as shown in **Figure 5**. The controls free OTf, OTf(SMZ), and gNP were almost inactive against *C. minutissimum* (**Figure 5A**) but showed weak activity against *P. acnes* and *C. albicans* (**Figures 5B** and **C**). Free SMZ showed moderate activity against the three strains tested. It should be noted that free OTf or OTf(SMZ) showed weak to moderate activity against skin pathogens, but OTf-gNP and OTf(SMZ)-gNP exhibited vigorous, dose-dependent bactericidal activity against the three strains.

While OTf(SMZ)-gNP was significantly potent bactericidal in a dose-dependent manner against *C. minutissimum* and *C. albicans* (**Figures 5A** and **C**), surprisingly, OTf-gNP showed slightly more vigorous activity than OTf(SMZ)-gNP against *P. acnes* (**Figure 5B**). Given this degree of dose-dependency, OTf-gNP appeared to serve as a potent antibacterial agent, becoming even more potent bactericidal when the capping OTf was loaded with the antibiotic SMZ (OTf(SMZ)-gNP). As shown in **Figure 6**, OTf(SMZ)-gNP also exhibited potent, dose-dependent bactericidal activity against the Gram-negative bacteria *Escherichia coli* K-12 (A) and *Salmonella enteritidis* (B). Interestingly, OTf-gNP exhibited relatively strong bactericidal activity against *Salmonella enteritidis,* although it was still less potent than OTf(SMZ)-gNP (**Figure 6B**).

OTf(SMZ) gold nanoparticles against drug-resistant *Salmonella*

We examined the bactericidal potency of OTf-gNP and OTf(SMZ)-gNP against the drug-resistant wild-type (WT) *Salmonella enteritidis* and its *tol*C-deleted mutant (Δ*tol*C). As shown in **Figure 7**, the wild-type *Salmonella* was highly resistant to OTf, OTf(SMZ), free SMZ and to the con-

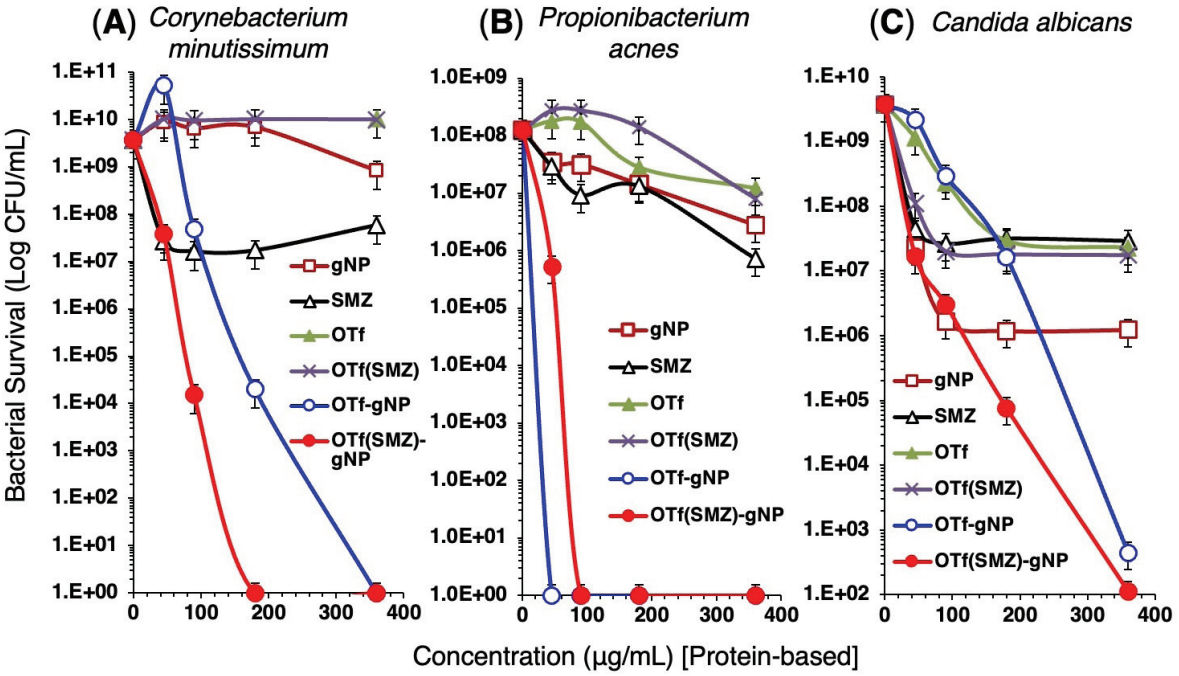

Figure 5. Bactericidal activity of various gNP formulations against skin pathogens *Corynebacterium minutissimum* (A), *Propionibacterium acnes* (B), and fungi *Candida albicans* (C). The assay was performed at different doses of gNPs, as well as free SMZ and OTf, at concentrations equivalent to their content in the respective formulations. The data is presented as log CFU/mL.

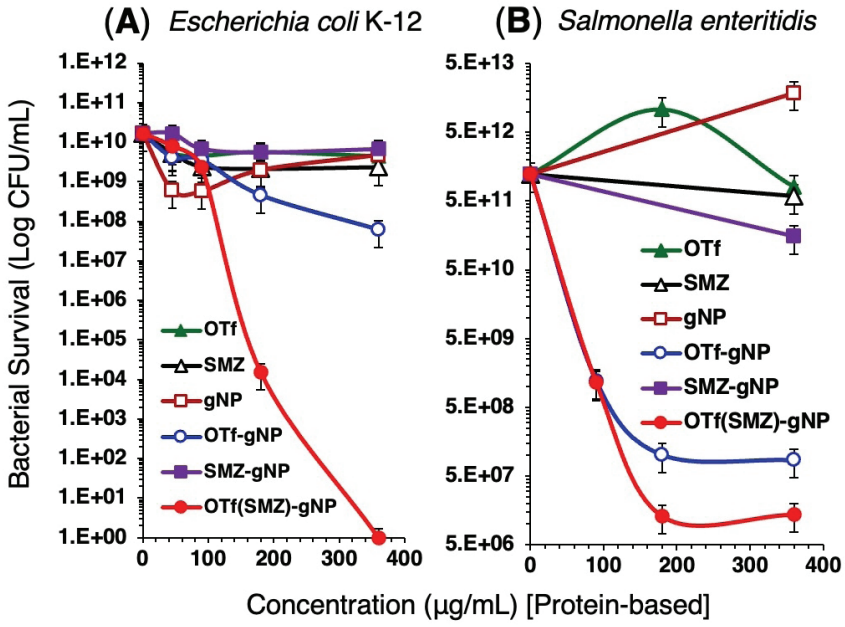

Figure 6. Bactericidal activity of various gNP formulations against Gram-negative *E. coli* (A) and *Salmonella enteritidis* (B). The assay was performed at different doses of gNPs as well as their free SMZ and OTf equivalents. The data is presented as log CFU/mL.

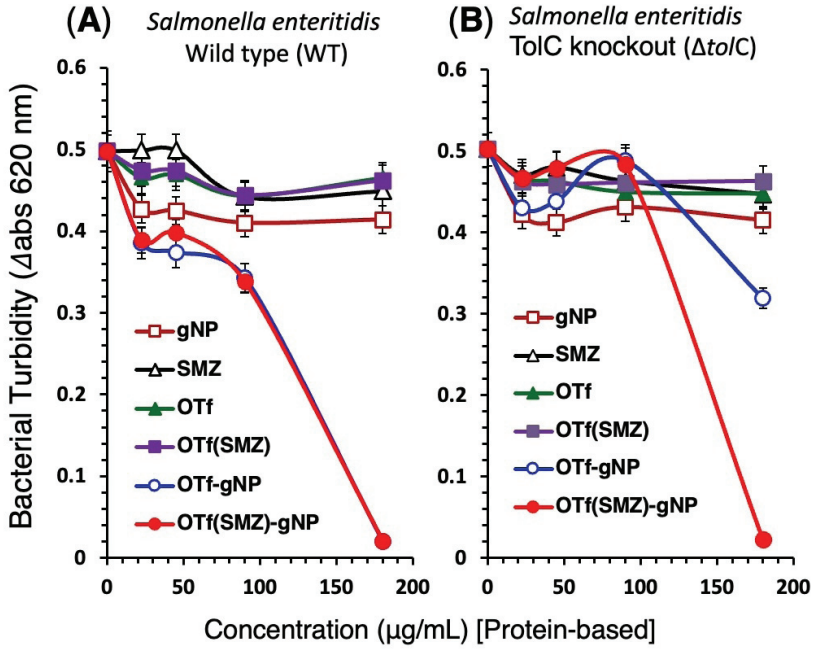

Figure 7. Antimicrobial activity of various gNP formulations against drug-resistant wild-type and *tol*C-deficient *Salmonella enteritidis*. The assay was performed against wild-type, WT (A) and *tol*C-deficient mutant, Δ*tol*C (B) strains at different doses of gNPs as well as their free SMZ and OTf equivalents. The data are presented as bacterial growth monitored at A620 nm.

trol nanoparticles (gNP), while it was sensitive to OTf-gNP and OTf(SMZ)-gNP (**Figure 7A**). Deletion of the *tol*C gene (Δ*tol*C) abolished the antibacterial effect of OTf-gNP against the wild-type (WT) *Salmonella* Enteritidis. Still, the bacteria remained significantly susceptible to OTf(SMZ)-gNP (**Figure 7B**). The results of **Figures 7A** and **B** suggest that OTf-capped gNP (OTf-gNP) is recognised and bound to TolC on the surface of wild-type *Salmonella* cells, where this physical contact effectively induces a killing effect. On the other hand, the bactericidal effect of OTf(SMZ)-gNP on *tol*C knockout *Salmonella* cells (**Figure 7B**) may be attributed to the high concentration of the antibiotic SMZ that is loaded onto the nano-formulation.

Facilitated OTf-gNP delivery of SMZ to intracellularly residing pathogens

The anti-infective effect of OTf(SMZ)-gNP on *S. aureus* (**Figure 8**) and *E. coli* (**Figure 9**) infecting HCT-116 cells intracellularly. The results were expressed as colony-forming units (CFU) per 10^6 cells. The free gNP showed a weak effect on the survival of the two intracellularly residing bacterial strains, comparable to mock-treated cells (Ctrl). The free OTf or SMZ exhibited moderate reduction of the intracellular bacterial survival of both *S. aureus* (**Figure 8A**) and *E. coli* (**Figure 9A**). While the OTf(SMZ) conjugate significantly decreased the survival of both strains, the OTf(SMZ)-gNP completely eradicated intracellular *S. aureus* (**Figure 8A**) and significantly reduced the intracellular *E. coli* (**Figure 9A**) within two hours of treatment. The OTf-gNP, lacking antibiotics, remarkably reduced intracellular bacterial survival of *S. aureus* (**Figure 8A**) but was less effective against *E. coli* (**Figure 9A**).

Subsequent post-hoc tests were conducted to determine which specific group comparisons were statistically significant. For S. aureus, the OTf(SMZ)-gNP and OTf-gNP treatments resulted in complete eradication or a remarkable reduction of intracellular bacteria. Both treatments were found to be statistically significant when compared to all other groups (Ctrl, free gNP, free OTf, and free SMZ), with a p-value < 0.05. OTf(SMZ) conjugate treatment also resulted in a statistically significant reduction of bacterial survival compared to the control group (Ctrl) and free gNP, with a p-value < 0.05. Free OTf and free SMZ treatments showed a statistically significant

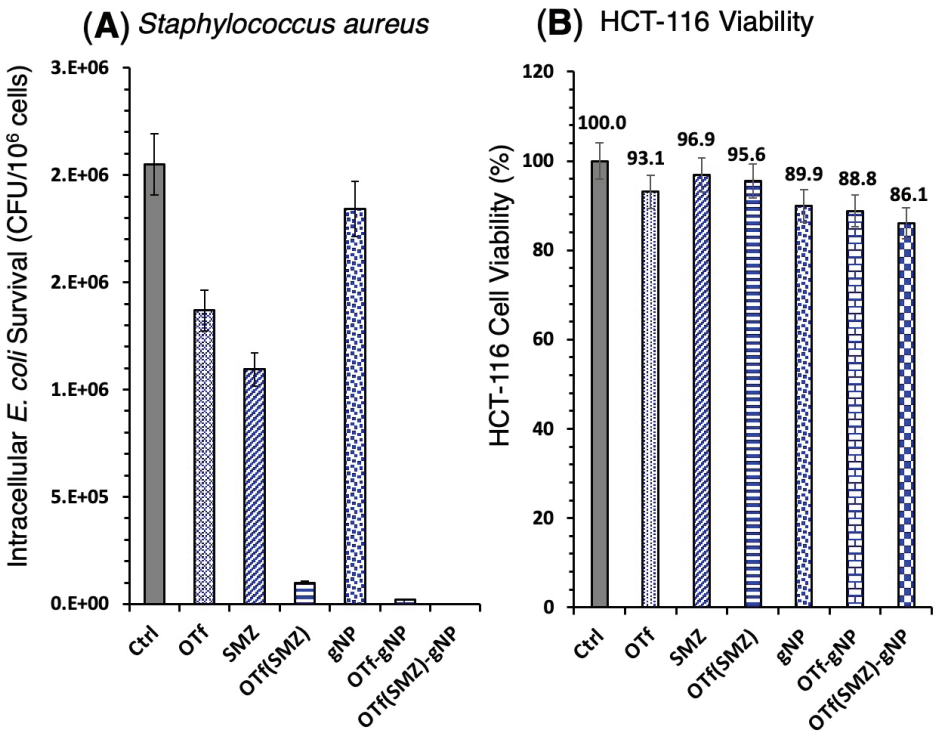

Figure 8. Recovery of *Staphylococcus aureus* (A) from the infected HCT-116 cells and viability of pre-infected HCT-116 cells (B). Cells were inoculated with 5 log cfu bacteria for 2 hours, then the extracellular bacteria were killed by gentamicin. Cells were washed and then treated with various gNP formulations or their OTf and SMZ equivalents and incubated for two hours at 37˚C under 5% CO_2. The HCT-116 cells were disrupted with Triton X-100, and the intracellular viable count was determined on TSA agar. Ctrl is cells treated with sterile distilled water. Values are expressed as the mean CFU per 10^6 cells of total protein from two experiments. Viability of pre-infected HCT-116 cells and subsequently treated with the indicated derivative for two hours was quantified by CellTiter Blue assay, and bars represent the mean with $n = 3$.

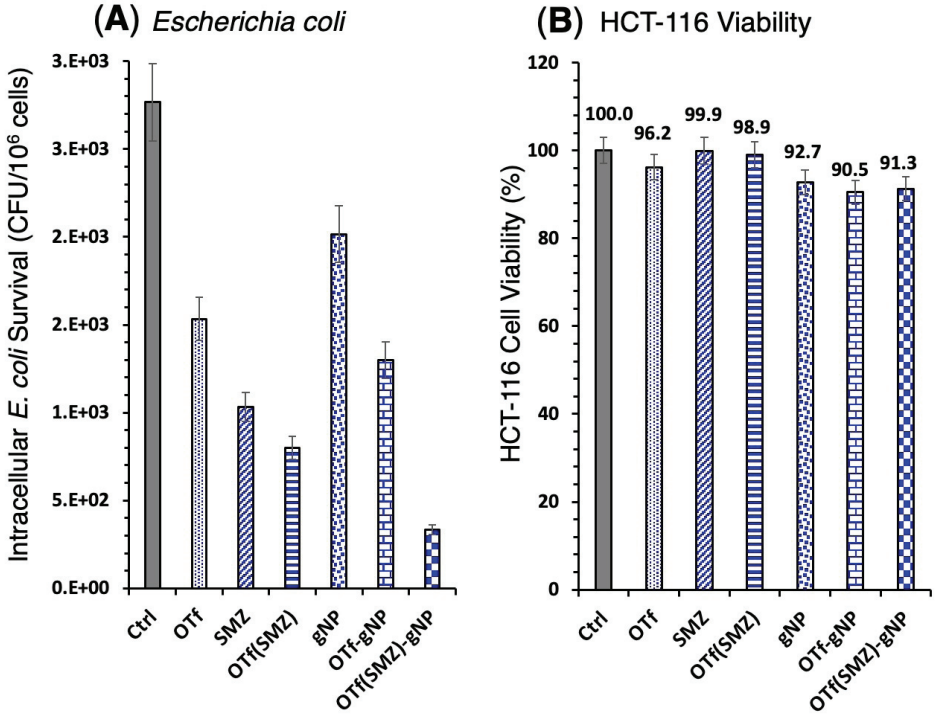

Figure 9. Recovery of *E. coli* (A) from the infected HCT-116 cells and viability of pre-infected HCT-116 cells (B). Experiments were carried out as shown in the Figure. 8.

moderate reduction in bacterial survival compared to the control group (Ctrl), with a p-value < 0.05. The difference between the OTf(SMZ)-gNP and OTf-gNP groups was not statistically significant ($p > 0.05$), suggesting a similar high level of efficacy for both treatments against *S. aureus* infections.

As for E. *coli*, OTf(SMZ)-gNP treatment resulted in a statistically significant reduction of intracellular bacteria compared to all other groups, with a p-value < 0.05. OTf-gNP treatment also caused a decrease in bacterial survival, but this effect was less significant compared to the OTf(SMZ)-gNP group, with a p-value < 0.05. OTf(SMZ) conjugate treatment led to a statistically significant decrease in bacterial survival compared to the control group (Ctrl), with a p-value < 0.05. Free OTf and free SMZ treatments exhibited a statistically significant moderate reduction in bacterial survival compared to the control group (Ctrl), with a p-value < 0.05. These results confirm that the OTf(SMZ)-gNP and OTf-gNP treatments are significantly more effective than the other treatments, with a notable difference in efficacy against *E. coli,* where the addition of SMZ in the OTf(SMZ)-gNP conjugate provides a significantly enhanced effect. The higher susceptibility of *S. aureus* to OTf-gNP compared to *E. coli* is a key finding, possibly due to the presence of transferrin receptors on the *S. aureus* surface.

To evaluate the effect of nanoparticle formulations on infected HCT-116 cells, cell viability was determined using the CellTiter Blue assay. As shown in **Figures 8B** and **9B**, OTf, SMZ, and their conjugate OTf(SMZ) exhibited negligible to weak inhibition of HCT-116 cell growth, while gNP, OTf-gNP and OTf(SMZ)-gNP showed moderate growth inhibition of HCT-116 cells. After treating for 2 hr with *S. aureus*-infected HCT-116, the growth inhibitory rates of OTf, SMZ, OTf(SMZ), gNP, OTf-gNP and OTf(SMZ)-gNP were 93.1%, 96.9%, 95.6%, 89.9%, 88.8% and 86.1%, respectively. Post-hoc analysis using Tukey's HSD test revealed several statistically significant differences in growth inhibition rates of HCT-116 cells. Specifically, the nanoparticle formulations, gNP ($p = 0.012$), OTf-gNP ($p = 0.008$), and OTf(SMZ)-gNP ($p = 0.003$), showed significantly lower growth inhibitory rates compared to the non-nanoparticle formulations OTf, SMZ, and OTf(SMZ). There were no statistically significant differences found among the nanoparticle formulations themselves or among the non-nanoparticle formulations. After treating HCT-116 cells infected with *E. coli* for 2 hours, the growth inhibitory rates of OTf, SMZ, OTf(SMZ), gNP, OTf-gNP, and OTf(SMZ)-gNP were 96.2%, 99.9%, 98.9%, 92.7%, 90.5%, and 91.3%, respectively. A Tukey's HSD post-hoc test showed a statistically significant difference between the nanoparticle formulations and the non-nanoparticle formulations. Specifically, the growth inhibition rates of gNP ($p < 0.001$), OTf-gNP ($p < 0.001$), and OTf(SMZ)-gNP ($p < 0.001$) were significantly lower than those of OTf, SMZ, and OTf(SMZ). These results suggest that while all tested formulations exhibit some level of growth inhibition, the nanoparticle-based formulations are consistently less effective at inhibiting cell growth in both *S. aureus*- and *E. coli*-infected HCT-116 cells.

Discussion

In this study, we prepared gold nanoparticles (gNPs) capped with the OTf molecule alone (OTf-gNP) or OTf preloaded with the water-insoluble antibiotic SMZ [OTf(SMZ)-gNP] as a potent antimicrobial formula. The gNPs were synthesised by the redox method using citrate as an environmentally friendly reducing agent. The OTf molecule was adsorbed onto the gNPs, increasing the diameter of gNPs from 15.72 nm to 19.32 nm with OTf and to 19.76 nm with SMZ-OTf conjugate. Both the OTf(SMZ)-gNP and OTf-gNP gold nanoparticles demonstrated potent antimicrobial activity against various bacterial isolates at low doses. At a dose of 180 µg/mL, OTf(SMZ)-gNP caused 2.43-log, 5.19-log, 3.30-log, 6.03-log and 4.98-log reduction of *S. epidermidis, S. aureus, S. zooepidermicus, E. coli* and *Salmonella enteritidis*, respectively. On the other hand, OTf-gNP at the same dose caused 2.06-log, 2.37-log, 1.31-log, 1.56-log and 4.08-log reduction of *S. epidermidis, S. aureus, S. zooepidermicus, E. coli* and *Salmonella enteritidis*, respectively. OTf(SMZ)-gNP exhibited more potent antimicrobial activity than OTf-gNP, particularly against the skin pathogens *S. epidermidis*, *S. aureus*, *C. minutissimum* and the fungus *C. albicans*. OTf(SMZ)-gNP caused 9.56-log, 8.09-log, and 4.69-log reduction at 180 µg/mL of the skin pathogens *C. minutis-*

simum, P. acnes and C. albicans, respectively. At the same time, OTf-gNP at the same dose caused 5.26-log, 8.09-log and 2.35-log reduction of *C. minutissimum, P. acnes and C. albicans,* respectively. The differences in antibacterial action between OTf(SMZ)-gNP and OTf-gNP are related to the intrinsic properties of gNPs or the nature of the cell membrane and biomolecules within the microorganism [18].

The gNPs serve as carriers for the antibacterial OTf, resulting in significantly stronger antimicrobial effects when OTf is loaded with the antibiotic SMZ. Notably, the formulated nanoparticles exhibited excellent activity against drug-resistant *Salmonella*. Both *Escherichia coli* K-12 and *Salmonella enteritidis* are known to possess outer membrane components such as TolC involved in the AcrAB-TolC multidrug resistance channel [19,20]. TolC is involved in the export of siderophores, components with a high affinity for iron [21,22], and has been reported to be activated when contacted with transferrin [23,24]. Therefore, we. Conducted tests to determine whether TolC plays a role in the bactericidal activity of OTf-capped nanoparticles. Both OTf(SMZ)-gNP and OTf-gNP caused complete inhibition (96% inhibition) of the drug-resistant wild-type *Salmonella*. Interestingly, OTf(SMZ)-gNP exhibited the same growth inhibitory efficacy (96% inhibition), but OTf-gNP showed significantly reduced inhibitory (36% inhibition) of the *tol*C-deleted *Salmonella* mutant (Δ*tol*C). These results align with a previously reported study on the mechanism of NPs affecting antibiotic resistance [25]. It has been revealed that NPs can be densely packed on the outer membrane, and some of them penetrate and kill bacterial cells, where the effects depend on the size of the NPs and the nature of the molecules at the surface of the bacterial cell [10]. Conceivably, the gold nano-formulation concentrated SMZ on the bacterial cell wall by passing the drug efflux pump (TolC) through passive delivery. The OTf on the surface of OTf-gNP interacted multivalently with the bacterial surface receptors, thereby inducing bacterial growth inhibitory action. Particularly, gNPs are known to enhance the permeability of bacterial cell membranes [8,10,11,26]. According to a study on Gram-negative bacteria, nanoparticles effectively eliminate multidrug-resistant isolates, and their action is mediated by the TolC efflux pump 23, [19,23,27]. This conclusion is supported by the observation that gNP alone exhibited significantly weaker antibacterial activity than the OTf(SMZ)-gNP and OTf-gNP nano-formulations. The superior antibacterial activities of OTf(SMZ)-gNP and OTf-gNP against *S. aureus* and skin pathogens *C. minutissimum* and *P. acne* could contribute to the treatment of skin wound healing.

Interestingly, both OTf(SMZ)-gNP and OTf-gNP exhibited excellent antimicrobial activity against the yeast/fungal *C. albicans*. Notably, the OTf(SMZ)-gNP demonstrated a more potent effect at considerably lower doses, indicating the contribution of SMZ loaded in the formulation. A recent study on the mechanisms of gNPs against *Candida* demonstrated that gNPs can interact with the H^+-ATPase-mediated proton pump, thereby disrupting the proton gradient and resulting in yeast/fungal cell death [9]. We previously demonstrated that OTf modulates the proton pump when expressed in the yeast *Pichia* [28]. Additionally, its N-terminal derived peptide can dissipate the microbial transmembrane electrochemical potential [29], thus disturbing the proton gradient. Hence, the effective activity of OTf(SMZ)-gNP against *C. albicans* is due to the disturbance of the membrane gradient by OTf and the known ability of gNPs to interact with the H^+-ATPase-mediated proton pump [9], thereby propagating the effect of SMZ. Our results, therefore, boosted the candidacy of OTf-gNP as a potent antimicrobial agent and OTf(SMZ)-gNP as a promising antibiotic-targeting carrier for treating skin infections and yeast/fungal Candidiasis.

Apart from the above antimicrobial activities, both OTf(SMZ)-gNP and OTf-gNP demonstrated significant antibacterial effects on the drug-resistant wild-type *Salmonella enterica* carrying the *tol*C resistance gene. The TolC is an outer membrane component of the AcrAB-TolC multidrug resistance channel, involved in siderophore export, thus allowing *Salmonella* to survive in iron-restricted and antibiotic environments [21,22]. An in-depth study has shown that the *tol*C promoter is activated upon contact with transferrin [19]. The sensitivity of wild-type *Salmonella* to OTf-gNP, while Δ*tol*C *Salmonella* was resistant, suggests that OTf acts as a modulator of the AcrAB-TolC efflux pump, which disrupts the growth of wild-type *Salmonella* [30].

In contrast, the intense antimicrobial action of OTf(SMZ)-gNP against both wild-type and Δ*tol*C *Salmonella* indicates that its effect is independent of the TolC channel, likely occurring through multi-mobility diffusion into the cell membrane [8,11]. However, the mechanism remains to be further confirmed.

We have explored the efficiency of OTf-gNP as a drug carrier to facilitate the delivery of the water-insoluble antibiotic SMZ into HCT-116 cells intracellularly infected with *S. aureus* or *E. coli*. The nano-formulations OTf(SMZ)-gNP and OTf-gNP potently caused the death of both intracellular bacterial strains, whereas the bacteria were poorly sensitive to pure gNP and weakly susceptible to free OTf or SMZ. In our recent work, we demonstrated the effective binding and internalisation of OTf into HCT-116 cells through transferrin receptor (TfR)-mediated uptake [5]. The higher susceptibility of intracellular *S. aureus* to OTf-gNP compared to *E. coli* may be due to the unique presence of transferrin receptor (TfR) on the peptidoglycan surface of *S. aureus* [31,32]. The significant reduction in both intracellular bacteria observed after exposure to OTf(SMZ)-gNP and OTf-gNP compared to OTf or SMZ suggests the roles of TfR-mediated uptake and direct diffusion. This mechanism facilitated the delivery and enhanced accumulation of the antibiotic (SMZ) or the gold nanoparticles in the cytosol of infected cells.

The present study thus demonstrates a novel approach for utilising an abundant egg protein, OTf, as a drug-targeting molecule through TfR-mediated endocytosis, achieving higher efficacy and minimal toxicity, thereby intervening in intracellular bacterial infections.

Conclusions

In this study, the synthesis of sulfamethoxazole (SMZ)-loaded ovotransferrin (OTf) gold nanoparticles [OTf(SMZ)-gNP] has been established via exploiting the reducing power of citrate. The OTf(SMZ)-gNP nanoparticles were irregularly shaped, with a quasi-spherical morphology within the nano-size range. Loading SMZ onto the OTf molecule and then capping the gNP significantly enhanced its antibacterial potency against both Gram-positive and Gram-negative bacteria, as well as the fungal *C. albicans* at much lower doses than the pure individual components, SMZ, OTf or gNPs. This nano-formulation demonstrated a remarkable antibacterial efficacy against drug-resistant *Salmonella* and enabled the delivery of OTf(SMZ) through TfR-mediated endocytosis into the intracellular milieu of infected cells. These results pave the way for the development of other gNP-based antibiotic formulations to combat the rising problem of drug resistance. Although gNPs are nontoxic [26], further in vivo studies are needed to examine the bioavailability, toxicity, and kinetics of OTf(SMZ)-gNP, which are necessary to assess its clinical applicability.,

Abbreviations

OTf	Ovotransferrin
SMZ	Sulfamethoxazole
gNP	Gold nanoparticles
OTf-gNP	Ovotransferrin capped gold nanoparticles
OTf(SMZ)	Ovotransferrin complex with sulfamethoxazole
OTf(SMZ)-gNP	Gold nanoparticles capped OTf(SMZ)
SMZ-gNP	Sulfamethoxazole-loaded gNP
CFU	Colony forming unit
TSA	Trypticase soy agar
PBS	Phosphate buffered saline
WT	Wild-type *Salmonella* Enteritidis
Δ*tol*C	*tol*C-deleted mutant *Salmonella* Enteritidis

Disclosures

Author Contributions

"Conceptualization, H.R. Ibrahim; methodology, H.R. Ibrahim and T. Kubo; formal analysis, H.R. Ibrahim and T. Kubo; investigation, H.R. Ibrahim; resources, H.R. Ibrahim; data curation, H.R. Ibrahim and T. Kubo; writing—original draft preparation, H.R. Ibrahim; writing—review and editing, H.R. Ibrahim; visualization, H.R. Ibrahim; supervision, H.R. Ibrahim; project administration, H.R. Ibrahim. All authors have read and agreed to the published version of the manuscript."

Funding

This research received no external funding

Acknowledgements

The Authors would like to thank the Research Support Centre of Kagoshima University for TEM analysis and the Department of Pathology, Bacteriology and Avian Diseases, Faculty of Veterinary Medicine, Ghent University, Belgium, for the wild-type and *tol*C-deficient mutant *Salmonella Enteritidis* strains.

Conflicts of Interest

The authors declare that they have no conflicts of interest.

References

1. Ovung A, Bhattacharyya J. Sulfonamide drugs: structure, antibacterial property, toxicity, and biophysical interactions. Biophys Rev. 2021;13:259–272. https://doi.org/10.1007/s12551-021-00795-9.
2. Tačić A, Nikolic V, Nikolic L, Savic I. Antimicrobial sulfonamide drugs. Adv Technol. 2017;6:58–71. https://doi.org/10.5937/savteh1701058T.
3. Jia X, Li S, Wang Y, Wang T, Hou X. Adsorption Behavior and Mechanism of Sulfonamide Antibiotics in Aqueous Solution on a Novel MIL-101(Cr)@GO Composite. J Chem Eng Data. 2019;64:1265–1274. https://doi.org/10.1021/acs.jced.8b01152.
4. Dibbern DA, Montanaro A. Allergies to sulfonamide antibiotics and sulfur-containing drugs. Ann Allergy Asthma Immunol Off Publ Am Coll Allergy Asthma Immunol. 2008;100:91–100; quiz 100–103, 111. https://doi.org/10.1016/S1081-1206(10)60415-2.
5. Ibrahim HR, Tatsumoto S, Ono H, Van Immerseel F, Raspoet R, Miyata T. A novel antibiotic-delivery system by using ovotransferrin as targeting molecule. Eur J Pharm Sci Off J Eur Fed Pharm Sci. 2015;66:59–69. https://doi.org/10.1016/j.ejps.2014.10.005. Cited: in: : PMID: 25315410.
6. Ibrahim HR, Miyawaki D, Miyata T. Ovotransferrin as a novel drug-targeting molecule for cancer chemotherapy. J Stem Cell Res Med. 2020;5:1–8. https://doi.org/10.15761/JSCRM.1000141.
7. Jana S, Sen KK, Gandhi A. Alginate Based Nanocarriers for Drug Delivery Applications. Curr Pharm Des. 2016;22:3399–3410.
8. Debets VE, Janssen LMC, Šarić A. Characterising the diffusion of biological nanoparticles on fluid and cross-linked membranes. Soft Matter. 2020;16:10628–10639. https://doi.org/10.1039/D0SM00712A.
9. Tian E-K, Wang Y, Ren R, Zheng W, Liao W. Gold Nanoparticle: Recent Progress on Its Antibacterial Applications and Mechanisms. J Nanomater. 2021;2021:2501345. https://doi.org/10.1155/2021/2501345.
10. Nakamura H, Watano S. Direct Permeation of Nanoparticles across Cell Membrane: A Review. KONA Powder Part J. 2018;35:49–65. https://doi.org/10.14356/kona.2018011.
11. Hsieh C-L, Spindler S, Ehrig J, Sandoghdar V. Tracking Single Particles on Supported Lipid Membranes: Multimobility Diffusion and Nanoscopic Confinement. J Phys Chem B. 2014;118:1545–1554. https://doi.org/10.1021/jp412203t.
12. Methner U, al-Shabibi S, Meyer H. Experimental oral infection of specific pathogen-free laying hens and cocks with Salmonella enteritidis strains. Zentralblatt Vet Reihe B J Vet Med Ser B. 1995;42:459–469. https://doi.org/10.1111/j.1439-0450.1995.tb00737.x. Cited: in: : PMID: 8578920.
13. Datsenko KA, Wanner BL. One-step inactivation of chromosomal genes in Escherichia coli K-12 using PCR products. Proc Natl Acad Sci. 2000;97:6640–6645. https://doi.org/10.1073/pnas.120163297.
14. Mezghich S. Photochemical Degradation of the Antimicrobial Sulfamethoxazole upon Solar Light Excitation: Kinetics and Elucidation of Byproducts Using LC/ ESI+/MS2 Technique. Mass Spectrom Purif Tech [Internet]. 2016;
15. Saptarshi SR, Duschl A, Lopata AL. Interaction of nanoparticles with proteins: relation to bio-reactivity of the nanoparticle. J Nanobiotechnology. 2013;11:26. https://doi.org/10.1186/1477-3155-11-26.
16. Mekuye B. The Impact of Size on the Optical Properties of Silver Nanoparticles Based on Dielectric Function. In: Ameen S, Akhtar MS, Jiménez-Suárez A, Seisdedos G, editors. Nanotechnol Nanomater Annu Vol 2024 [Internet]. Rijeka: IntechOpen; 2023 [cited 2025 Feb 13]. Available from: https://doi.org/10.5772/intechopen.113976.
17. Sørensen LK, Khrennikov DE, Gerasimov VS, Ershov AE, Polyutov SP, Karpov SV, Ågren H. Nature of the Anomalous Size Dependence of Resonance Red Shifts in Ultrafine Plasmonic Nanoparticles. J Phys Chem C. 2022;126:16804–16814. https://doi.org/10.1021/acs.jpcc.2c03738.
18. Hoshyar N, Gray S, Han H, Bao G. The effect of nanoparticle size on in vivo pharmacokinetics and cellular interaction. Nanomed. 2016;11:673–692. https://doi.org/10.2217/nnm.16.5.
19. Horiyama T, Yamaguchi A, Nishino K. TolC dependency of multidrug efflux systems in Salmonella enterica serovar Typhimurium. J Antimicrob Chemother. 2010;65:1372–1376. https://doi.org/10.1093/jac/dkq160. Cited: in: : PMID: 20495209.
20. Yousefian N, Ornik-Cha A, Poussard S, Decossas M, Berbon M, Daury L, Taveau J-C, Dupuy J-W, Đorđević-Marquardt S, Lambert O, et al. Structural characterization of the EmrAB-TolC efflux complex from E. coli. Biochim Biophys Acta BBA - Biomembr. 2021;1863:183488. https://doi.org/10.1016/j.bbamem.2020.183488.
21. Li K, Chen W-H, Bruner SD. Microbial siderophore-based iron assimilation and therapeutic applications. Biometals Int J Role Met Ions Biol Biochem Med. 2016;29:377–388. https://doi.org/10.1007/s10534-016-9935-3. Cited: in: : PMID: 27146331.
22. Ratledge C, Dover LG. Iron metabolism in pathogenic bacteria. Annu Rev Microbiol. 2000;54:881–941. https://doi.org/10.1146/annurev.micro.54.1.881. Cited: in: : PMID: 11018148.

23. Zgurskaya HI, Krishnamoorthy G, Ntreh A, Lu S. Mechanism and Function of the Outer Membrane Channel TolC in Multidrug Resistance and Physiology of Enterobacteria. Front Microbiol. 2011;2:189. https://doi.org/10.3389/fmicb.2011.00189. Cited: in: : PMID: 21954395.
24. Wang Z, Fan G, Hryc CF, Blaza JN, Serysheva II, Schmid MF, Chiu W, Luisi BF, Du D. An allosteric transport mechanism for the AcrAB-TolC multidrug efflux pump. eLife. 2017;6:e24905. https://doi.org/10.7554/eLife.24905. Cited: in: : PMID: 28355133.
25. Xu Y, Li H, Li X, Liu W. What happens when nanoparticles encounter bacterial antibiotic resistance? Sci Total Environ. 2023;876:162856. https://doi.org/10.1016/j.scitotenv.2023.162856.
26. Enea M, Peixoto de Almeida M, Eaton P, Dias da Silva D, Pereira E, Soares ME, Bastos M de L, Carmo H. A multiparametric study of gold nanoparticles cytotoxicity, internalization and permeability using an in vitro model of blood-brain barrier. Influence of size, shape and capping agent. Nanotoxicology. 2019;13:990–1004. https://doi.org/10.1080/17435390.2019.1621398.
27. Mishra M, Kumar S, Majhi RK, Goswami L, Goswami C, Mohapatra H. Antibacterial Efficacy of Polysaccharide Capped Silver Nanoparticles Is Not Compromised by AcrAB-TolC Efflux Pump. Front Microbiol. 2018;9:823. https://doi.org/10.3389/fmicb.2018.00823. Cited: in: : PMID: 29780364.
28. Ibrahim HR, Hozono A, Fukami M, Shaban MA, Miyata T. Expression of Ovotransferrin Enhances Tolerance of Yeast Cells toward Oxidative Stress. J Agric Food Chem. 2013;61:6358–6365. https://doi.org/10.1021/jf401152e.
29. Ibrahim HR, Sugimoto Y, Aoki T. Ovotransferrin antimicrobial peptide (OTAP-92) kills bacteria through a membrane damage mechanism. Biochim Biophys Acta. 2000;1523:196–205. https://doi.org/10.1016/s0304-4165(00)00122-7. Cited: in: : PMID: 11042384.
30. Allgood Samual C., Su Chih-Chia, Crooks Amy L., Meyer Christian T., Zhou Bojun, Betterton Meredith D., Barbachyn Michael R., Yu Edward W., Detweiler Corrella S. Bacterial efflux pump modulators prevent bacterial growth in macrophages and under broth conditions that mimic the host environment. mBio. 2023;14:e02492-23. https://doi.org/10.1128/mbio.02492-23.
31. Modun B, Kendall D, Williams P. Staphylococci express a receptor for human transferrin: identification of a 42-kilodalton cell wall transferrin-binding protein. Infect Immun. 1994;62:3850–3858. https://doi.org/10.1128/iai.62.9.3850-3858.1994. Cited: in: : PMID: 8063401.
32. van Dijk MC, de Kruijff RM, Hagedoorn P-L. The Role of Iron in Staphylococcus aureus Infection and Human Disease: A Metal Tug of War at the Host—Microbe Interface. Front Cell Dev Biol [Internet]. 2022;10.